

## Experimental study of the statistics of slipping events in solid friction

S. Ciliberto and C. Laroche

Ecole Normale Supérieure de Lyon, Laboratoire de Physique, C.N.R.S, URA 1325, 46, Allée d'Italie, 69364 Lyon, France

Received 20 September 1994 - Accepted 1 February 1995 - Communicated by D. Sornette

**Abstract.** The statistics of the stick-slip motion is studied in two experiments, where elasticity is distributed either on a surface or on a volume. The rough surface is realised by embedding steel spheres in an elastic substrate whereas the volume is constituted by several layers of rubber spheres. Both systems produce a complex dynamics characterized by power law with non-trivial exponents in the distribution of the amplitude of the slipping events and in the power spectra of the friction force time evolution. The dependence of the results on the system size is also studied.

### 1 Introduction

Solid friction has been widely considered as an important mechanism to understand the physics of earthquakes (Scholz 1990, Turcotte 1992). Many of the mathematical models, where this problem has been studied can be derived by the original one of Burridge and Knopoff (1967), which is based on the stick slip dynamics of blocks connected by springs, and sliding on a surface with a given friction law (for a recent review see Carlson et al. 1994). This kind of stick-slip motion has been also studied using cellular automata (Bak et al. 1988, Nakanishi 1990, Crisanti et al. 1992, Olami et al. 1992, Feder and Feder 1991). All of these models are characterized by a loading period where the system accumulates energy and a slip period, "the earthquake", where part of this energy is released. The study of these models is useful to understand whether it is possible to reproduce the Gutenberg-Richter law (G.R.) for the number of occurrence  $N$  of earthquakes with a given moment  $E$ , specifically  $N(E) \propto E^{-B-1}$ . We recall that for real earthquakes the average value of  $B$  is around 1. There are only a few numerical simulations where the G-R law is satisfied till the maximum energy (Sousa Vieira 1992, Knopoff et al. 1992, Olami et al. 1992). In general the  $N(E)$ , obtained from the models, presents an ano-

malous peak for large  $E$  (Carlson et al. 1994), that is to say the scaling is self-similar only for small earthquakes. These models are also important to investigate the relationship of self organized criticality (SOC) with earthquakes (Bak et al. 1988, Sornette and Sornette 1989, Sornette 1992).

In spite of the large amount of numerical data on the above mentioned models, there are only a few laboratory experiments (Feder and Feder 1991, Valette and Gollub 1993, Johansen et al. 1994) where the stick slip dynamics has been tested from the point of view of its statistical properties. In a very recent paper (Ciliberto and Laroche 1994) we have described an experiment on stick slip dynamics of two rough elastic surfaces. The underlying geophysical model, we had in mind, is the same of the Burridge Knopoff model for a fault (Burridge et al. 1967), and our experiment has been designed to analyse in some details the statistics of the slipping events of an elastic system composed by many different interacting parts. This system produces a dynamics similar to self organized critical state on a wide range of control parameters, namely loading speed and pressure. This means that both the amplitude of slip events, and the time interval between them have a power law distribution. We have shown that this complex behaviour is produced by the fact that the two elastic sliding surfaces were constructed by many different interacting parts. In this paper we describe an extension of this experimental study from two different points of view. The first one is related to the minimum number of independent asperities which are needed in order to produce a complex behaviour.

The second point, which we want to analyse, is that of the interaction of the two sliding surfaces. Indeed in real faults, which in a certain sense could be simulated by the stick-slip motion, the friction is mediated by the presence of many detritus of previous earthquakes. As a consequence we have done an experiment where the interaction of two very rough surfaces is mediated by se-

veral layers of small spheres. In this paper we describe under what conditions this system has a complex dynamics characterized by power law distributions with non-trivial exponents.

The paper is organized as following. In section 2) we describe the method used to construct the surfaces and the geometries used. In section 3) we summarize the statistical properties of the stick-slip dynamics of the different geometries. We also analyse how these properties change as a function of the number of interacting asperities. The results of the volume experiments are described in section 4). Finally the results are discussed in section 5).

## 2 The experimental set up

Several experiments with different geometries and different surfaces have been performed. Here we described two of them, the linear and the volume ones. Other examples with rigid surfaces can be found in another paper ( Ciliberto and Laroche 1994).

### 2.1 The linear experiment

In the first experimental set up, shown in fig.1a), a linear geometry has been used. A slide is moved at constant speed  $V$  on a rough surface constructed with steel spheres emerging of 0.5 mm from a wood plate 180 cm long and 20 cm wide. The motion of the slide is kept straight by two lateral trucks which avoid the lateral motion. The force  $F(t)$  necessary to move the slide at constant speed is measured by a force transducer. The transducer signal suitably amplified and filtered is converted by a 16 bits A/D converter. The minimum detectable variation of the friction force  $F_f$  is about  $3 \cdot 10^{-2} N$ .

The normal force  $F_n$  acting on the surface of the slide can be changed by modifying the weight of the slide. Several slides are used in order to study the dependence on the system size and on the number of asperities. One  $9.5 \times 200 cm^2$  and the other  $9.5 \times 5 cm^2$ . The surface of the slide was constructed in the following way: First a rectangular hole of depth 1.5 mm is made on one of the slide surface. The hole covers almost all the slide surface except for a small frame 0.5 cm wide on the sides. We put inside this hole steel spheres of diameters 2 mm in such a way that the distance between sphere centers was about two diameters. Finally the hole was filled with silicon rubber. In this way an artificial surface with controlled roughness and elasticity is constructed. The maximum roughness is exactly 0.5 mm equal to the sphere diameter minus the depth of the groove. Furthermore each single sphere is rather free to move around its equilibrium position because of the elasticity of the rubber. We will call this surface soft surface to be distinguished from another type of surface which has been used in order to study the dynamics as a function of the

compliance of the matrix of spheres. The compliance was changed using glues with different elasticity. These tests have been done in an annular geometry ( Ciliberto and Laroche 1994) and the results will be not discussed here.

It is important to explain how the steel spheres actually move. By looking at fig.1 we see that the spheres are touching the bottom of the plate. Thus, when a sphere is pushed against an asperity of the opposite surface, it cannot pass over this asperity but it can only move transversely to the direction of the loading velocity in order to go around the obstacle. This has been verified by making a transparent slide and looking from above, with a video-camera, the motion of several spheres. This is useful also to estimate the maximum displacement of a sphere that is about 0.2 mm.

### 2.2 Physical properties of the surfaces and typical time scales

The stick-slip dynamics produced by the system described in the previous section has been studied as a function of the loading speed  $V$  and of the normal forces. The values of the applied parameters must be compared with those obtained using the physical properties of the experiment. The mass  $\mathcal{M}_s$  of the spheres is  $4 \cdot 10^{-5} Kg$  and the total number of spheres  $N_s$  is in between 150 and 600. The total mass  $\mathcal{M}_T$  involved is in the range 40 g to 2 Kg. With the total mass we indicate the sum of sphere masses plus that of the slide. The Young modulus  $E$  of the rubber where spheres are embedded is  $5 \cdot 10^5 N/m^2$ . Therefore, using as a typical length scale the sphere diameter  $d = 2 \cdot 10^{-3} m$ , the elastic constant  $k = E \cdot d$  is  $10^3 N/m$ . Two typical time scales can be defined, one based on the acceleration of  $\mathcal{M}_s$  and the other of  $\mathcal{M}_T$ :  $T_T = (\mathcal{M}_T/k)^{1/2}$  and  $T_s = (\mathcal{M}_s/k)^{1/2}$ . We find that  $T_s \simeq 2 \cdot 10^{-4} sec$  whereas  $T_T \simeq 3 \cdot 10^{-2} sec$ . As it will be discussed in section 3, this value of  $T_T$  is very close to the sliding time for the smallest events measured on the friction force, meaning that the motion is dominated by the total inertia. The damping time of the oscillation of  $\mathcal{M}_s$  and  $\mathcal{M}_T$  are of the same order of  $T_s$  and  $T_T$  respectively. This means that the system is over damped and oscillations are not allowed.

Another important time scale is  $T_V = d/V$  which corresponds to the time needed to move the plate of a characteristic length; we will see that this time corresponds to the loading time between two very large events.

The measured average friction coefficient of the artificial surface is  $\mu = 0.3$  and it increases as a function of  $V$ .

### 2.3 The volume experiment

We have done another experiment in order to study different interactions. The cross section of the experiment is shown in fig.1b. It is constructed by two annular ro-

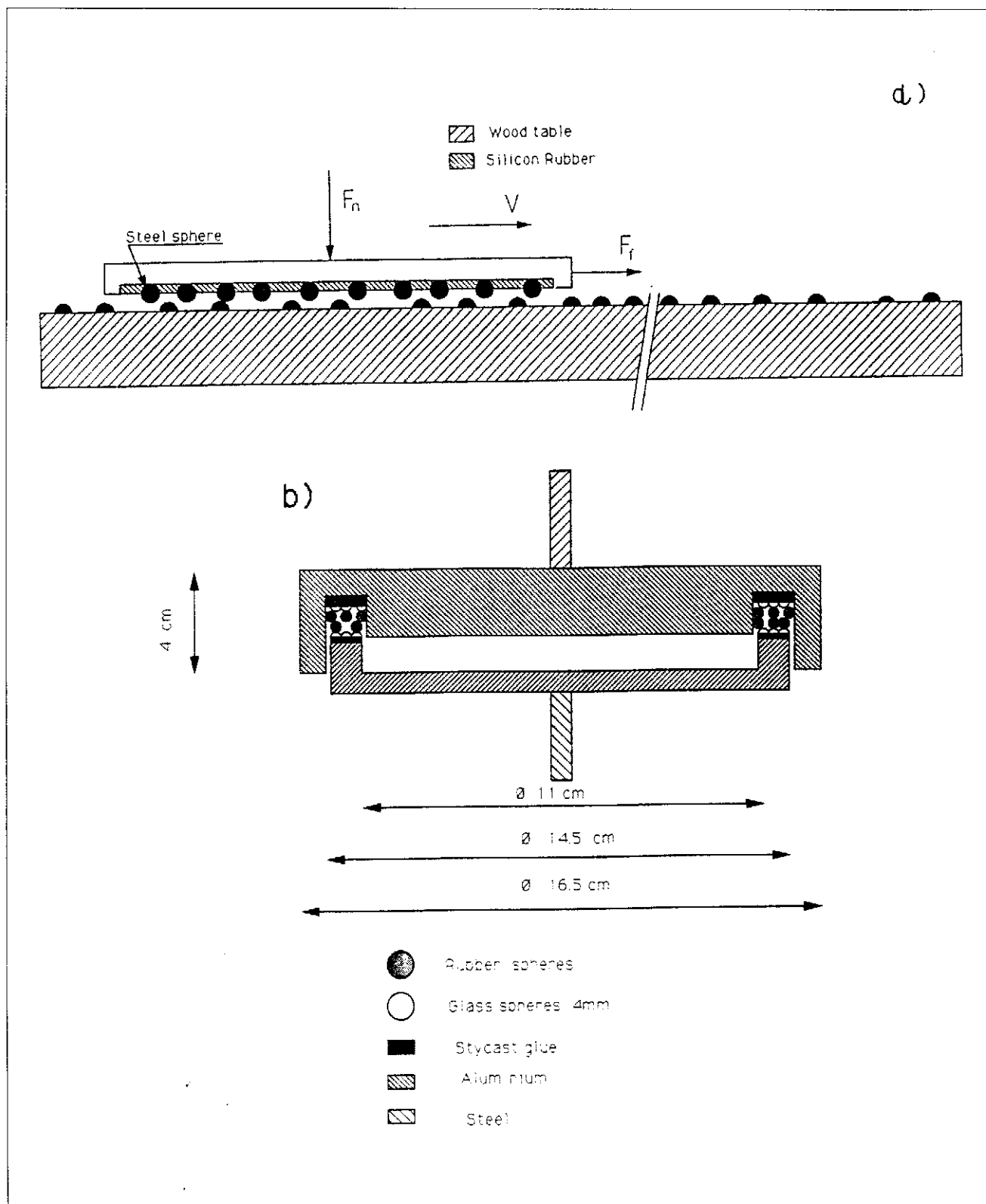


**Fig. 1.** Experimental apparatus. a) Cross section of the linear geometry experiment; the slide is moved at constant speed  $V$  and the friction dependent force  $F_f$  is measured by a force transducer. The wood table is 180 cm long. b) Cross section of the volume experiment. The bottom, disk is moved at constant angular speed and the torque necessary to keep the top disk fixed is measured.

ugh surfaces which were prepared similarly to the surface of the slide of the linear experiment described in section 2-a. The difference is that glass spheres (4 mm of diameter) are glued with a "stycast glue" which once is dried becomes very rigid, as a consequence the spheres are fixed rigidly on the disk surfaces. The bottom disk is moved at constant angular speed  $\Omega$  whereas the top disk is kept fixed. The main difference with respect to the annular experiment (Ciliberto and Laroche 1994) is that here, the bottom and top rough surfaces do not touch but a gap of a few millimeters is left between them. The two surfaces may interact by means of several layers of spheres (diameter 2mm) which fill the gap between the two surfaces. As can be seen in fig.1b there are an external and an internal cylindrical walls around the two annular rough surfaces in order to confine the layers of spheres. A strain gauge measures the torque necessary to keep the top disk fixed. Furthermore a micrometric device allows us to change the pressure with which the two disks are pushed one against the other.

Two different experiments were performed one with the volume filled with steel spheres and the other with the volume filled with rubber spheres and the results are discussed in section 3.

### 3 The statistical properties of stick slip

We summarize in Sect.3.1 and 3.2 the statistical properties of the stick slip dynamics in linear experiment (more details can be found in Ciliberto and Laroche 1994). In section 3.3 we analyse instead the dependence of results on the system size.

To analyse the statistics of the system we first record the force  $F(t)$  and an example for the linear case is shown in fig.2. We clearly distinguish loading cycles where the two surfaces are stuck and  $F(t)$  increases till time  $t_i$  where it reaches a relative maximum. At that point the slip period begins and lasts till time  $t_c$  where  $F(t)$  reaches a relative minimum and then it begins to increase again. We define the amplitude of the slip event as  $M(t_i) = F(t_i) - F(t_c)$ .

We can estimate the lateral displacements of spheres corresponding to the minimum  $M_{min}$  and maximum  $M_{max}$  value of  $M(t)$ . We fixed  $M_{min}$  at the minimum detectable variation of the  $F(t)$ , that is  $3 \cdot 10^{-2} N$  in our apparatus (see Sect.2.1). Assuming that minimum events are produced by only one sphere we find that  $u_{min} = M_{min}/k = 3 \cdot 10^{-2} mm$  which is very reasonable value because is about 1/7 of the maximum displacement we have measured with a video-camera (see Sect.2.1). Displacements of the spheres smaller than  $u_{min}$  are of course possible but are not detected by our experimental set up. In contrast  $M_{max} = 6 N$ , as one can see in fig.2. Thus  $u_{max} = M_{max}/k = 6 mm$ , which is about 30 times the maximum displacement of the spheres, which we have observed with the camera (see Sect.2.1). There-

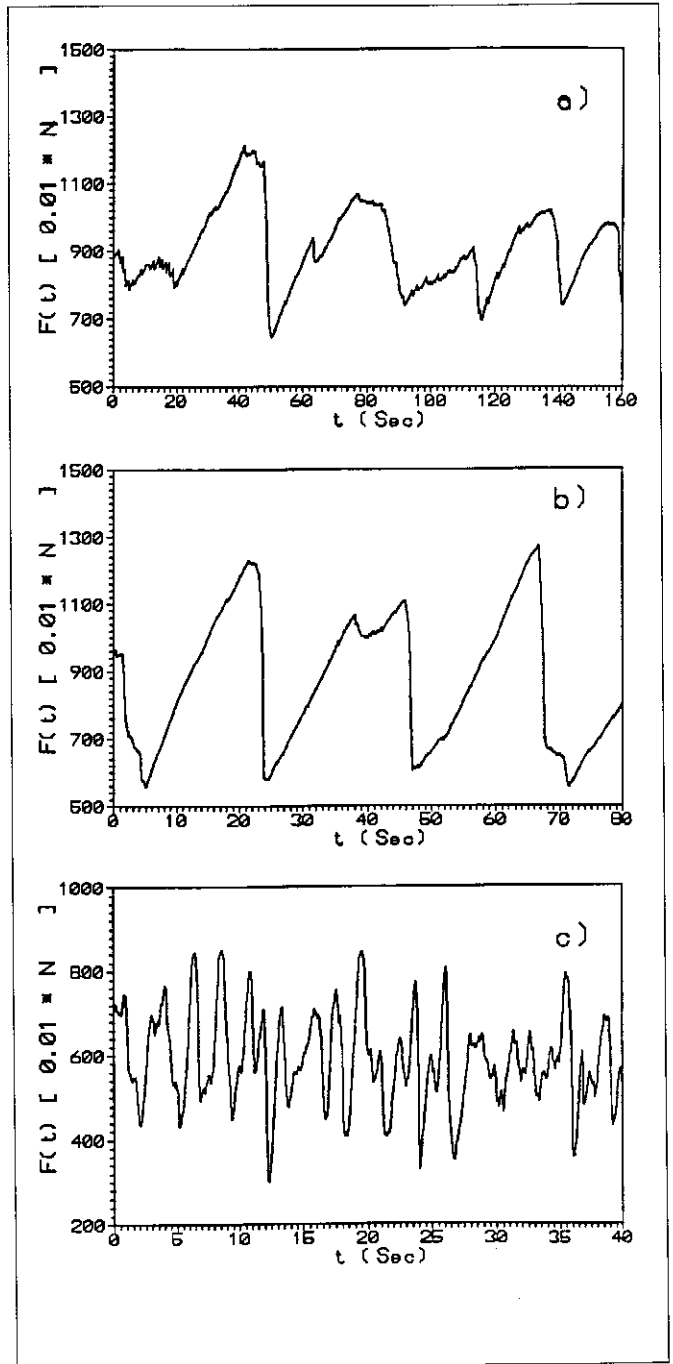


Fig. 2. Friction force versus time for different loading speeds. a)  $V = 0.04 mm/sec$ ; b)  $V = 0.1 mm/sec$ ; c)  $V = 1.25 mm/sec$ .

fore one deduces that the largest events are produced by an ensemble of at least 30 spheres, which are displaced of about 0.2mm. This is of course rather unreasonable because it is more natural to think that many spheres, about 100 or more, are displaced of less than 0.2mm. This estimation of  $u_{max}$  and  $u_{min}$ , although rather qualitative, is useful in order to show that small events implies a small number of spheres whereas large events

imply a large number of asperities. Notice that  $u_{min}/T_T$  identify a characteristic sliding velocity  $V_c \simeq 1mm/sec$ . Indeed we will see in the next section that all interesting statistical features disappear when  $V > V_c$  that is when loading speed become comparable to sliding speed. This behaviour is clearly visible in fig.2c where the loading periods lasts almost the same of the sliding periods

### 3.1 Probability distribution of slipping event amplitude

We measure the probability distribution function  $P(M)$  of  $M$  finding a transition to a power law distribution for small velocities  $V$ . At least  $10^4$  events have been recorded to construct  $P(M)$  which is shown in Fig.3a. We see that at high velocities  $P(M)$  presents just a large plateau with an exponential cut-off whereas at small velocities a power law appear with an exponent  $\gamma$  which is increasing for decreasing  $V$  and it reaches the value of about 2 for  $V \rightarrow 0$ . This is seen in fig.3b where the exponents  $\gamma$  of the power laws are reported as a function of  $V$ . (the points corresponding to the annular geometry described in Ciliberto and Laroche 1994 are also shown).

### 3.2 Power spectra

In fig.4 the power spectra of  $F(t)$  for two different  $V$  are shown. They have been obtained as an average of 100 spectra of the  $F(t)$  signal. We clearly see an important difference in the two spectra. At high  $V$  the spectrum is broadened with a sharp cut off. In contrast at slow  $V$  the spectrum decays in  $f^{-3}$  for at least one order of magnitude. This means that the derivative of  $F(t)$  decays in  $f^{-1}$ . Indeed by looking at the shape of the signal in fig.2a) we understand that the largest contribution to the derivative of  $F(t)$  is coming from the fast decreasing parts (the slip phase) whose amplitude  $M$  has a power law distribution as we have seen in fig.4. We found that for slow speeds also the probability distribution  $P(\tau)$  of the time  $\tau$  between to successive events of any amplitude is a power law (see fig.5). Specifically for  $V = 0.01cm/s$   $P(\tau) \simeq 1/\tau$ . In contrast at  $V = 1.25mm/sec$   $P(\tau)$  is simply broadened with no specific feature. Thus one conclude that at small  $V$  not only  $P(M)$  has a power law dependence but also the power spectra and  $P(\tau)$ .

### 3.3 Dependence on the system size

We have shown ( Ciliberto and Laroche 1994) that the cut-off of  $P(M)$ , i.e. the amplitude of largest events, depends on the normal force, and on the system size. Furthermore we demonstrated that the statistical beha-

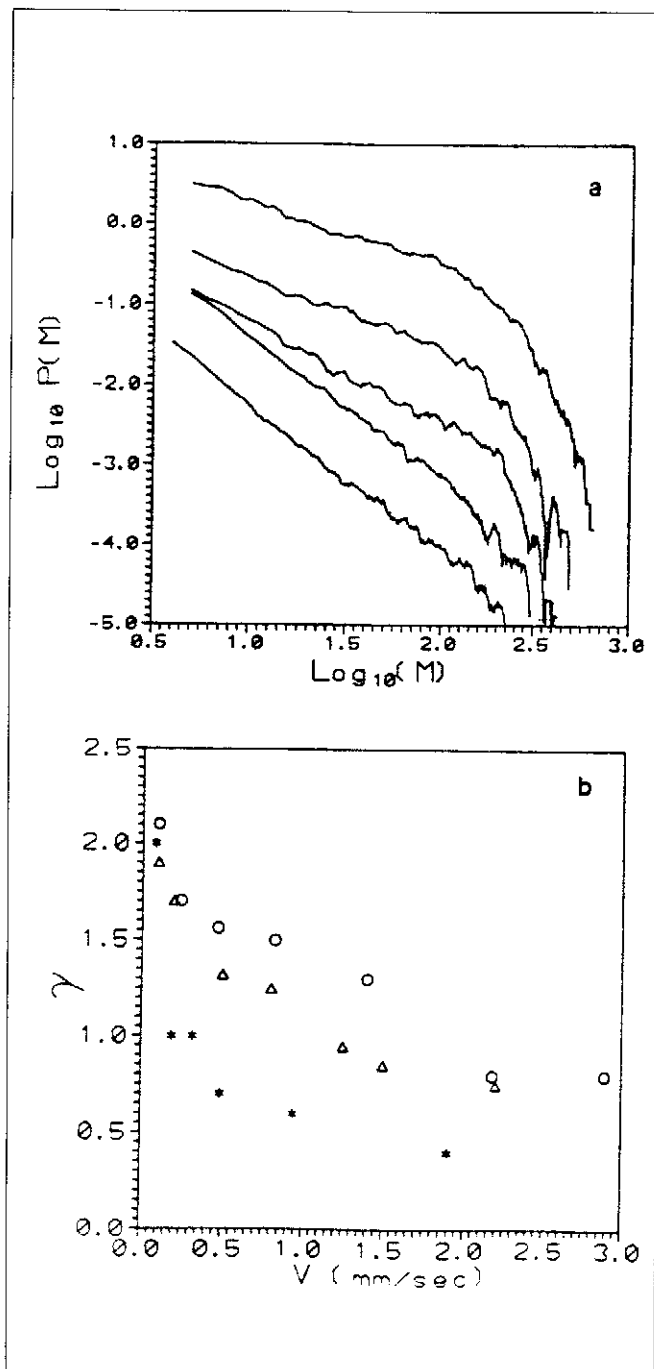


Fig. 3. Event size distribution  $P(M)$  for different loading speeds. Starting from the bottom curve the corresponding  $V$  are,  $0.1mm/sec$ ,  $0.2mm/sec$ ,  $0.5mm/sec$ ,  $1.5mm/sec$  and  $2.2mm/sec$ . The vertical scale is arbitrary because the curves have been shifted in order to clearly show their shapes on the same graph. b) Exponent of the power laws of  $P(M)$  as a function of the loading speed for different normal forces and different experimental set up (see also Ciliberto, Laroche 1994).  $\circ$  and  $\Delta$  correspond to the interaction in the disks and linear experiment respectively. \* correspond to the soft-rigid case on the disk experiment.

viour is also determined by the compliance of the sphere array, that is when the system becomes too rigid the power law distributions are destroyed.

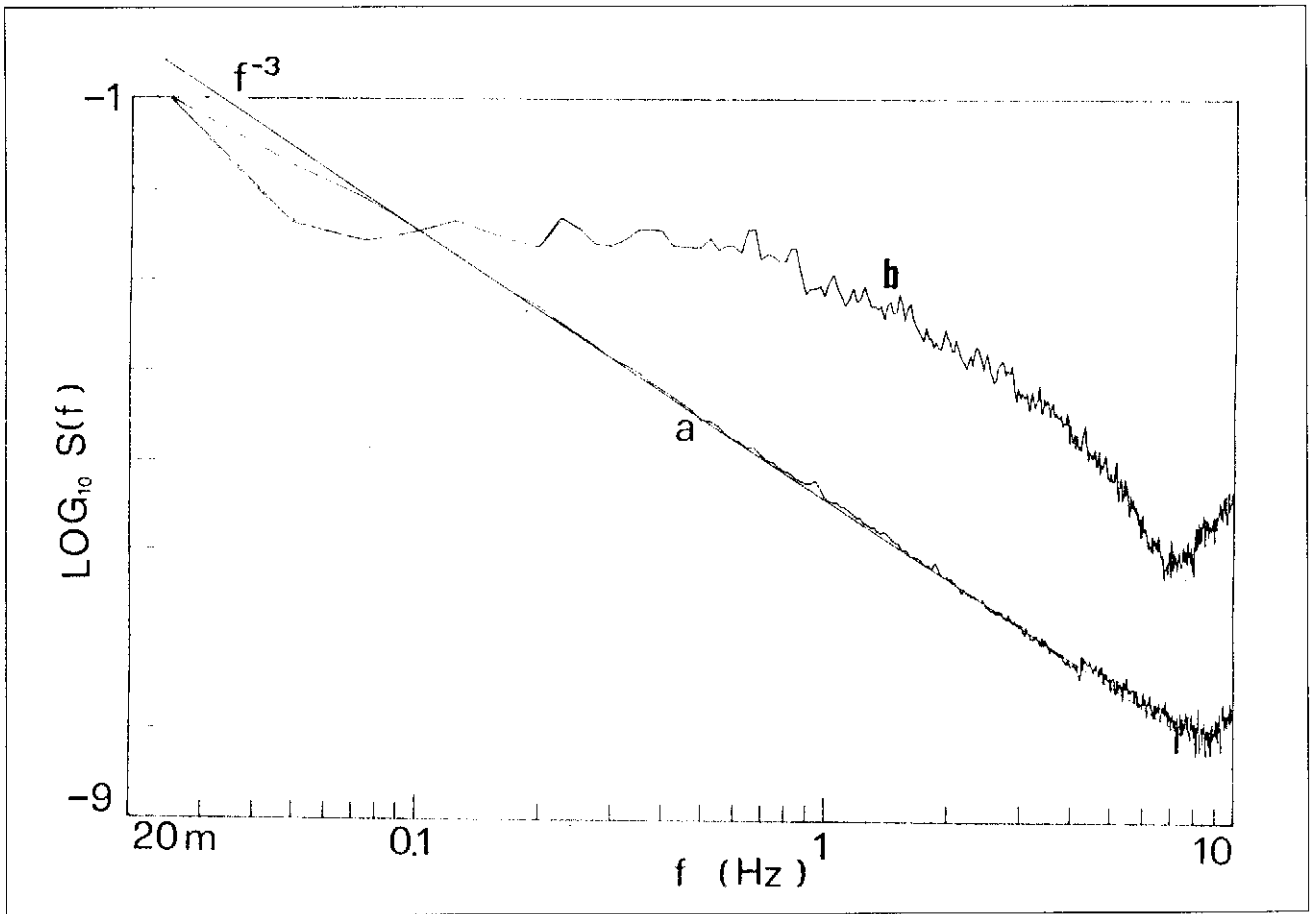


Fig. 4. Power spectra of  $F(t)$  for two different loading speeds  $V$ . a)  $V = 0.1 \text{ mm/sec}$  and b)  $V = 1.25 \text{ mm/sec}$ .

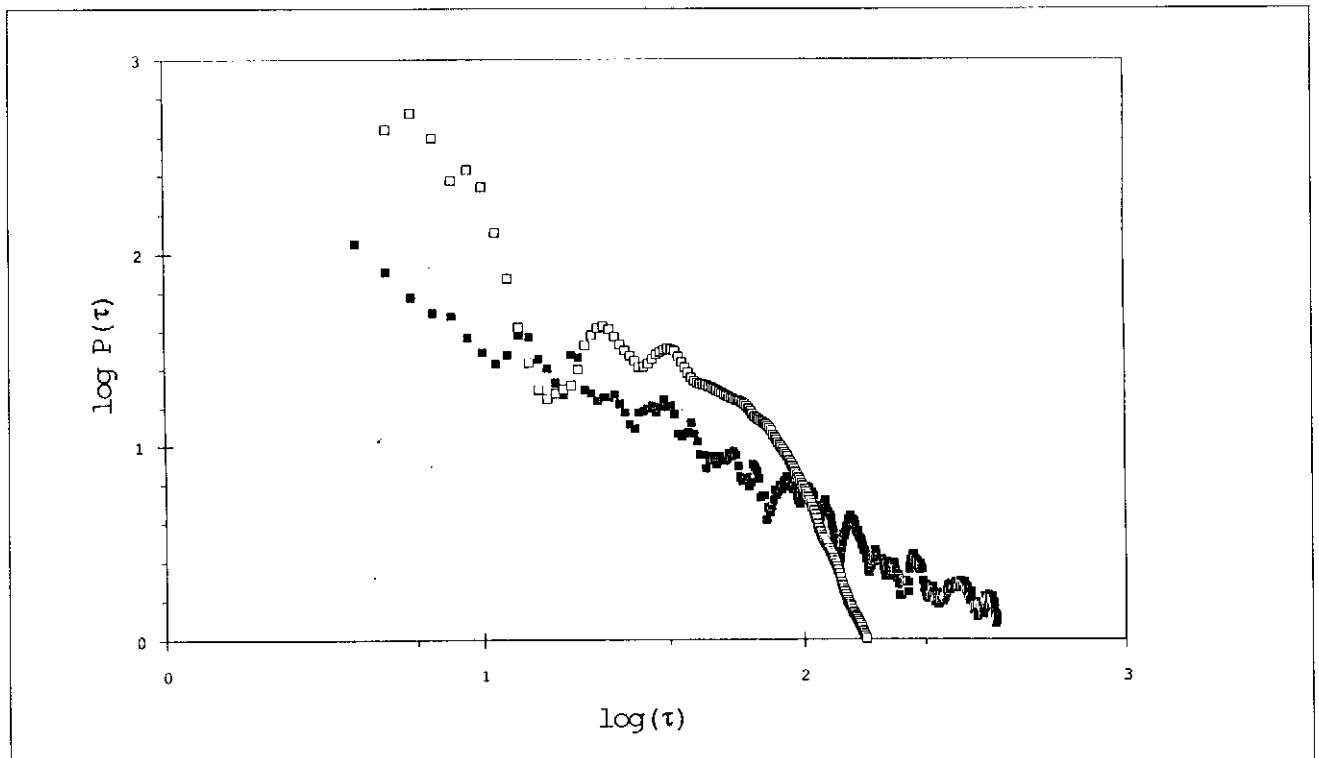


Fig. 5.  $P(\tau)$  for the same loading speeds of fig.4.

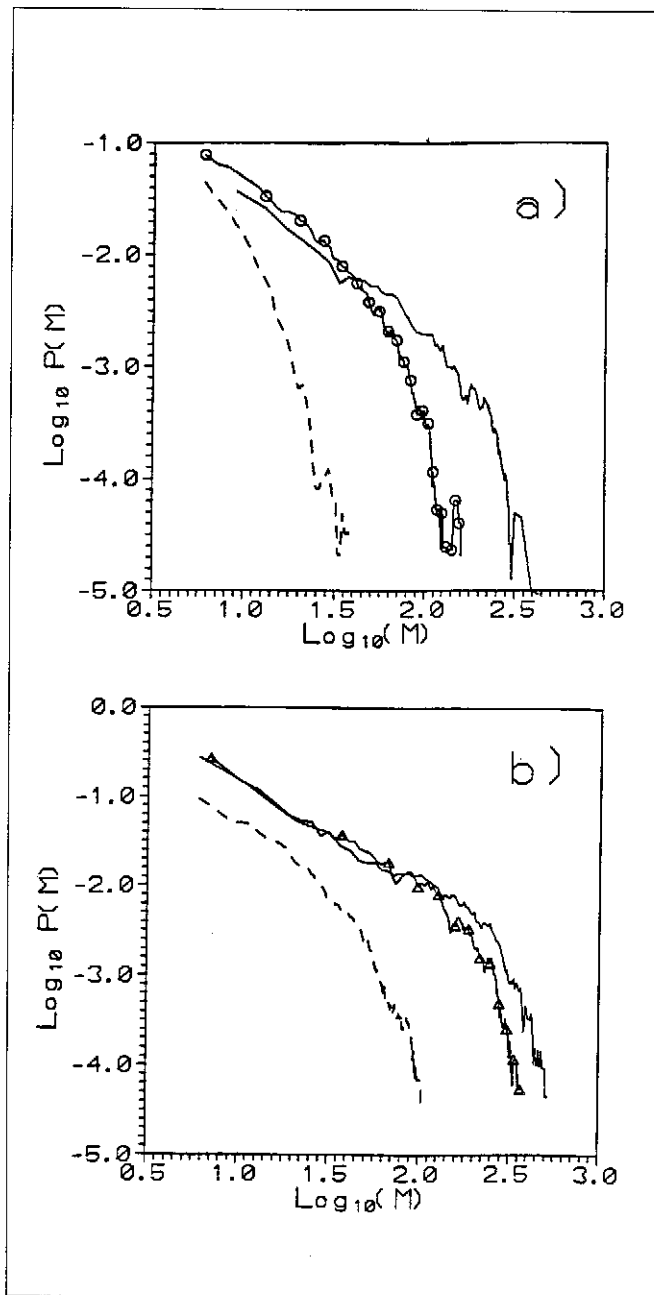


Fig. 6. Comparison of systems of different size as a function of  $\tilde{F} = F_n/N_s$  at  $V = 0.08\text{cm/s}$ . a)  $N_s = 150$  (continuous line  $\tilde{F} = 42.6\text{mN}$ ), (circles  $\tilde{F} = 16\text{mN}$ ), (dashed line  $\tilde{F} = 2.7\text{mN}$ ); b)  $N_s = 600$  (continuous line  $\tilde{F} = 21.3\text{mN}$ ), (triangles  $\tilde{F} = 16\text{mN}$ ), (dashed line  $\tilde{F} = 4.3\text{mN}$ );

In this section we describe the results of some new experiments which have been done in order to understand how many asperities (steel spheres in the linear experiment) are needed to have power law distributions. In other words we want to know the number of degrees of freedom in the systems which produce a complex behaviour. To do this we have used slides of different size and we constructed the elastic surfaces always with the same silicon glue keeping the same average surface density of

spheres in all of the slides. Indeed a relevant parameter, which controls the dynamics, is the normal force acting on each sphere which is about  $F_n/S$ , if the number of spheres per unit area is constant (here  $S$  is the total surface where the spheres are glued). This is the case also in numerical simulations (Carlson et al. 1994, Huang and Turcotte 1990, de Sousa Vicira 1992, Knopoff et al 1992, Schmitzbuhl et al 1993) where the normal force acting on each block is one of control parameters. In fig.6 we compare the results at  $V = 0.08\text{cm/s}$  obtained from two slides of different size one contains 600 spheres and the other 150. We have applied several normal forces. We clearly see that  $\tilde{F} = F_n/N_s$  has the effect of reducing the amplitude of the biggest events. We also notice that for the smallest slide when  $\tilde{F}$  is low all power laws disappear indicating that the degrees of freedom are not so large in order to construct power laws. Furthermore the large system produce power laws even for  $\tilde{F}$  smaller than the maximum used in the small slide. Thus one deduces that the smallest is  $F_n$ , the largest should be the number of spheres in order to get the complex behaviour that we have discussed sections 3a,3b. We want also to stress that the limit of 150 spheres and  $F_n = 0.4\text{N}$  is almost the experimental limit because below this value of  $\tilde{F}_n$  the slide is just jumping over the asperities without producing the stick slip motion.

Finally we have checked that the dependence on the system size, and on  $\tilde{F}$  of the maximum events  $M_{max}$  is roughly:  $M_{max} \propto N_s \tilde{F}$ . This equation has been obtained by defining  $M_{max}$  as the value of  $M$  where  $\log[P(M_{max})] = -4$ .

#### 4 The volume interaction

The idea was to check whether the stick slip dynamics could produce a complex behaviour, also when the interactions between the two sliding surfaces is done by means of a deforming volume. This experiment is certainly more close to the reality of the faults because the coupling layers can be seen has the detritus formed by the previous slips. Furthermore elastic waves can propagate also in the interaction volume, which is not the case when the coupling between the two sliding surfaces is direct. Using the experimental configuration described in Sect.2.2 we have performed two experiments one with the gap between the two surfaces filled with steel spheres the other with rubber spheres, that is to say with a small and with a large compliance. In both cases four layers of spheres has been inserted.

##### 4.1 Rubber sphere coupling

The Young modulus  $E$  of the rubber spheres was about  $7 \cdot 10^6 \text{N/m}^2$ . Therefore using as a typical length scale dc spheres diameter  $d = 4\text{mm}$ , we get for the elastic

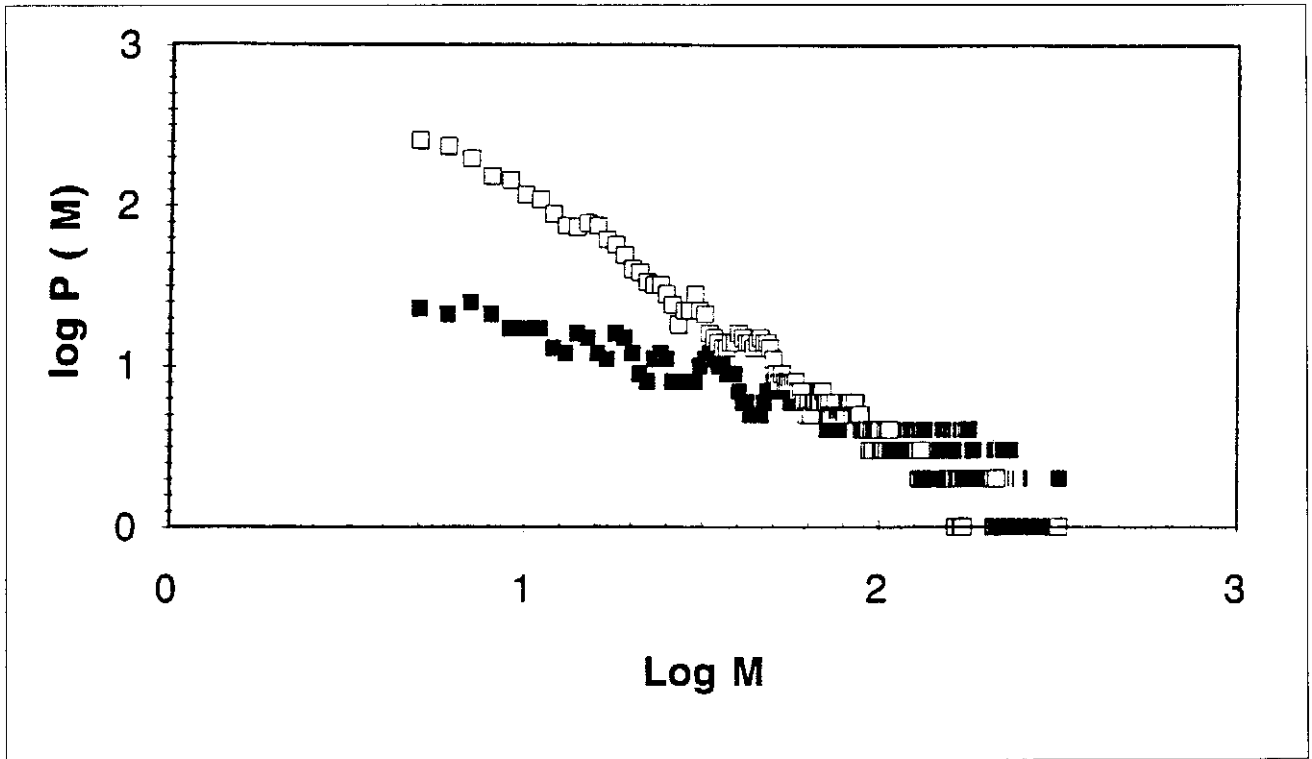


Fig. 7. Volume experiment with 4 layers of steel spheres.  $P(M)$  for two different loading speeds  $V = 0.035\text{mm/s}$  (squares), and  $V = 2.16\text{mm/sec}$  (black squares).

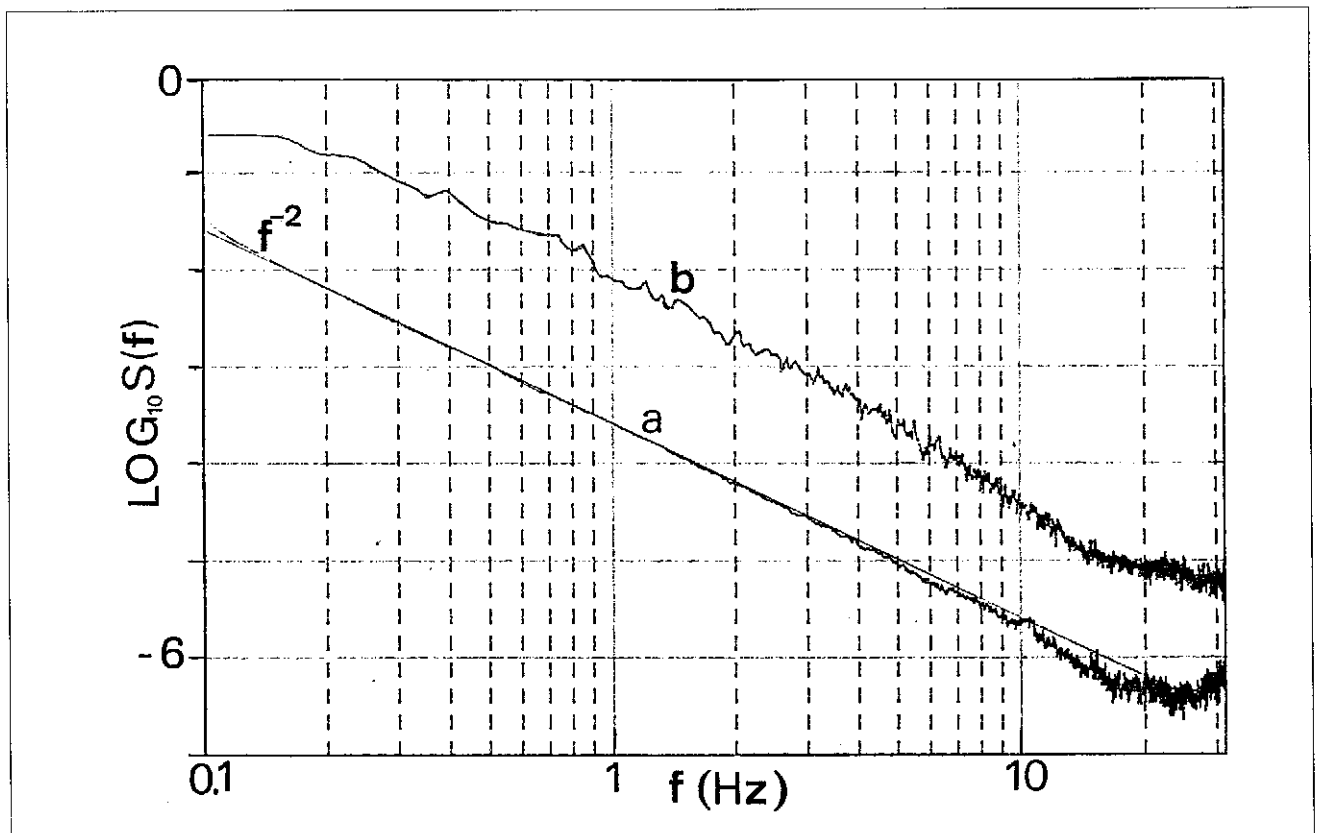


Fig. 8. Volume experiment with 4 layers of steel spheres. Power spectra of  $F(t)$  for the same loading speeds of fig.7.



constant  $k = E d = 28 \cdot 10^3 N/m$ . The typical time scales involved the total mass of the spheres and those of the disk, that is about  $2Kg$ . For the relaxation time we get  $T_T = (\mathcal{M}_T/k)^{1/2}$ , that is  $T_T = 8 \cdot 10^{-3}s$  which is about four times smaller than those for the linear experiment. However the slipping time were determined mainly by the elastic joint installed on the axis of the fixed disk. This joint had an elastic constant  $k' = 10^3 N/m$ . Thus the sliding time was very close to that computed for the linear experiment, and to those experimentally found in this volume experiment.

We do not show any plot for this experiment, because the dynamics of  $F(t)$  is very close to that described in Sect.3 for the linear experiment. Indeed we observe that not only  $P(M)$  is a power law but for slow loading speeds, but also the spectrum of  $F(t)$  has a power law  $f^{-3}$ .

#### 4.2 Steel sphere coupling

In this case the more elastic point of all the system is the elastic joint on the axis of the fixed disk. Thus the system has the same  $T_T$ . However due to the very small compliance of the coupling system, the dynamics of  $F(t)$  is very different in this case. Indeed for very slow loading speed  $P(M)$  has a power law but the shape of the curve is different as it can be seen in fig.7. This power law distribution disappears if the velocity is increased. Furthermore the spectra of  $F(t)$  has a trivial behaviour because it decays in  $f^{-2}$ . Spectra taken at two different speeds in the volume experiments are reported in fig.8. We clearly see that the spectrum a) has a behaviour as  $f^{-2}$ .

One of the possible reasons of different behaviours of the system filled with steel spheres and the one filled with rubber sphere is in the different arrangement of the spheres after many revolution of the disk. Indeed the steel spheres pile up forming regular array. In contrast rubber spheres, as they can deform, keep a random distribution during the dynamics.

The conclusion of these checks in the volume is that a complex dynamics is produced in a systems where the elasticity is distributed among many degrees of freedom.

### 5 Discussion and conclusions

In this paper we have extended the experimental results, described in a previous paper (Ciliberto and Laroche 1994), on the stick slip dynamics, produced by the friction of elastic surfaces which have an artificial and well defined roughness made of steel spheres. When one of these surfaces is moved on a similar one ( where spheres can be embedded in a soft or rigid glue), the spheres produce local interactions which are elastically coupled among them. Specifically, when the loading speed tends to zero the dynamics presents, for a wide range of

the control parameters, a complex dynamics. Indeed the event size distributions has a power law dependence with a cut-off which is a function of the system size. The frequency power spectra of the friction force decay algebraically with a non trivial exponent showing that the time evolution of the force is just the integral of a  $1/f$  noise. These features are similar to those presented by a self organized similar state, however it is difficult to conclude if this system can be included within those presenting SOC. Indeed we have seen that in our system as in many numerical ones, which present SOC, two control parameters must be changed in order to produce the complex behaviour. Specifically in Sect.3.1,3.2, we have seen that these two parameters are the number of asperities and the normal force. The latter is particularly important in our experiment, because it changes the interaction between the different asperities, thus producing large displacements of the spheres. In any case if one uses the general conditions for a system to evolve into SOC (R. Cafiero et al. 1995), one can state that the dynamics here described is certainly close to SOC, if the systems is composed by many different interacting parts.

In this paper we have also analysed a case where the two sliding surfaces are coupled by mean of several layers of spheres. If the coupling is done with rubber spheres the above mentioned complex behaviour is reproduced. In contrast when the layers are made of steel spheres the powers spectra have decay in  $f^{-2}$ .

The relevance of these kind of experiments in the study of earthquake statistics is doubtful, because friction is just an aspect of earthquakes (Scholz 1990, Sornette 1992). In contrast these experiments and the associated models can be more useful for understanding friction laws. In any case we have noticed in section 3 that the value of  $B$  obtained by the exponent  $\gamma$  of the power law in  $P(M)$  is  $0.5 < B < 1$  as for earthquakes. A more precise relationship between  $B$  and  $\gamma$  can be found by measuring the local displacement of the steel spheres, this will be also very important to study the mechanisms of friction laws.

As a conclusion, the most important result of this paper is that a very complex dynamics with many features of self organized criticality can be produced by the stick-slip dynamics provided that the system, either 3 or 2 dimensional, is composed by many different interacting parts and that the loading period is much smaller than the characteristic times of the system defined in terms of elastic constants. There were a few numerical examples in one and two dimensions ( de Sousa Vieira 1992, Knopoff et al. 1992, Olami et al. 1992) where this has been shown but no clear experimental evidences that this could be obtained on a laboratory scale.

*Acknowledgments.* We acknowledge C. Caroli, S. Fauve, F. Lund, M. de Sousa de Vieira, D. Sornette and J. P. Vilotte for useful discussion. This work has been partially supported by the "Region Rhône-Alpes".

## References

- P. Bak, C. Tang, K. Wiesenfeld, Self organized criticality, *Phys. Rev. A* 38, 364 (1988).
- R. Burridge, L. Knopoff, Model and Theoretical seismicity, *Bull. Seismol. Soc. Am.* 57, 341, 1967.
- R. Cafiero, V. Loreto, I. Pietronero, A. Vespignani, S. Zapperi, *Europhysics Lett.*, 29, 111, 1995
- J. M. Carlson, J.S. Langer, B. E. Shaw, Dynamics of earthquake faults, *Rev. Mod. Phys.*, 66, 657, 1994.
- S. Ciliberto, C. Laroche, Experimental evidence of self organized criticality in the stick-slip dynamics of two rough elastic surface *J. de Phys. I*, 4, 223, 1994.
- A. Crisanti, M.H. Jensen, A. Vulpiani, G. Paladin Strongly intermittent chaos and scaling in an earthquake model, *Phys. Rev. A* 46, 7363, 1992.
- H.J.S. Feder, J. Feder, Self-organized criticality in a Stick slip process, *Phys. Rev. Lett.* 66, 2669, 1991.
- B. Gutenberg, C. F. Richter, Magnitude and energy of earthquakes, *Bull. Seismol. Soc. Am.* 46, 105, 1956.
- J. Huang, D. Turcotte, Are earthquakes an example of deterministic chaos?, *Geophysical Research Lett.* 17, 223, 1990.
- L. Knopoff, J. A. Landoni, M. S. Abinac, Dynamical model of an earthquake fault with localization, *Phys. Rev A* 46, 7445, 1992.
- J. Johansen, P. Dimon, C. Ellegaard, J. S. Larsen, H. H. Rugh Dynamic phases in a spring block system, *Phys. Rev. E* 48, 4779, 1993.
- H. Nakanishi, Cellular automaton model of earthquakes with deterministic dynamics, *Phys. Rev. A* 41, 7086, 1990.
- Z. Olami, H.J. S. Feder, K. Christensen, Self organized criticality in a continuous non conservative cellular automaton modeling of earthquakes, *Phys. Rev. Lett.* 68, 1244, 1992.
- J. Schmitbuhl, J. P. Vilotte, S. Roux, Propagative macrodislocation modes in an earthquake fault model, *Europhysics Lett.* 21, 375, 1993.
- G. H. Scholz, *The Mechanics of earthquakes and faulting*. Cambridge University Press 1990.
- A. Sornette, D. Sornette, Self organized criticality of earthquakes, *Europhys. Letters* 9, 197, 1989.
- D. Sornette, Critical phase transitions made self organized criticality: a dynamical system feedback, *J. Physique* 2, 2089, 1992.
- M. de Sousa Vieira, Self organized criticality in a deterministic mechanical model, *Phys. Rev. A* 46, 6288, 1992.
- D. L. Turcotte, *Fractal and Chaos in Geology and Geophysics*. Cambridge University Press 1992.
- D. P. Valette, J. P. Gollub, Spatiotemporal dynamics due to the stick slip friction in an elastic membrane system, *Phys. Rev. A*, 47, 820, 1993.